J. Membrane Biol. 145, 33–47 (1995)

The Journal of
Membrane
Biology

Discrete and Reversible Vacuole-like Dilations Induced by Osmomechanical Perturbation of Neurons

C. Reuzeau*, L.R. Mills[2], J.A. Harris, C.E. Morris[1]

[1]Neurosciences, Loeb Institute, Ottawa Civic Hospital, 1053 Carling Ave, Ottawa, Ontario, Canada K1Y 4E9
[2]Playfair Neurosciences Unit, Toronto Western Hospital, Toronto, Ontario, Canada M5T 2S8

Received: 15 June 1994/Revised: 16 August 1994

Abstract. In cultured *Lymnaea stagnalis* neurons, osmolarity increases (upshocks) rapidly elicited large membranous dilations that could be dislodged and pushed around inside the cell with a microprobe. Subsequent osmolarity decreases (downshocks) caused these vacuole-like dilations (VLDs) to disappear. Additional upshock/downshock perturbations resulted in repeated appearance/disappearance (formation/reversal) of VLDs at discrete sites. Confocal microscopy indicated that VLDs formed as invaginations of the substrate-adherent surface of the neuron: extracellular rhodamine-dextran entered VLDs as they formed and was expelled during reversal. Our standard VLD-inducing perturbation was: 2–4 min downshock to distilled water, upshock to normal saline. However, a wide range of other osmotic perturbations (involving osmolarities up to 3.5× normal, perturbations with or without Ca^{2+}, replacement of ions by sucrose) were also used. We concluded that mechanical, not chemical, aspects of the osmo-mechanical shocks drove the VLD formation and reversal dynamics and that extracellular Ca^{2+} was not required.

Following a standard perturbation, VLDs grew from invisible to their full diameter (>10 μm) in just over a minute. Over the next 0.5–3 hr in normal saline, neurons recovered. Recovery eliminated any visible VLDs and was accompanied by cytoplasmic turmoil around the VLDs. Recovery was prevented by cytochalasin B, brefeldin A and *N*-ethylmaleimide but not by nocodazole. In striking contrast, these drugs did not prevent repeated VLD formation and reversal in response to standard osmo-mechanical perturbations; VLD disappearance during reversal and during recovery are different.

The osmo-mechanical changes that elicited VLDs may, in an exaggerated fashion, mimic tension changes in extending and retracting neurites. In this context we postulate: (a) the trafficking or disposition of membrane between internal stores and plasma membrane is mechanosensitive, (b) normally, this mechanosensitivity provides an "on demand" system by which neurons can accommodate stretch/release perturbations and control cell shape but, (c) given sudden extreme mechanical stimuli, it yields VLDs.

Key words: Membrane dynamics — Osmotic perturbations — Mechanical stress — Cell adhesion — Cytomechanics — Rhodamine-dextran

Introduction

Insertion of the new plasma membrane required for neurite outgrowth occurs over the entire neuron (Popov et al., 1993). Neuronal topology is potentially unstable, with large expanses of membrane forming long slender branches, each experiencing unique local stresses. Neurons must, therefore, possess a means of locally adjusting membrane area in response to local tension. Findings which suggest that insertion and retrieval could be tension sensitive include: tension is maintained as neurites change length and shape (Bray, 1992); a requisite for neurite outgrowth is that the growth cone exert pulling tension (Lamoureux, Buxbaum & Heidemann, 1989; Heidemann & Buxbaum, 1994); a neurite between a tethered soma and growth cone adjusts its length in response to experimentally altered tension (Campenot, 1984); membrane capacitance and area increase then decrease when neurons swell then shrink (Wan, Harris & Morris, 1995).

* *Present address:* Biology Department, Washington University, St Louis, MO 63130-4899

Correspondence to: C. Morris

Direct relations between neurite tension and the rates of membrane insertion and retrieval have not been established, but evidence from plant cells (Wolfe, Dowgert & Steponkus, 1985) and from an epithelial tissue suggests that membrane area adjustments may be mechanosensitive. Capacitance measurements of bladder epithelium indicate that cell surface area responds to tension; stretch-then-release stimuli (either mechanical or osmotic) induce insertion-then-retrieval of membrane at the apical surface (Lewis & de Moura, 1982).

In extending and retracting growth cones, membrane is cycled through special endocytic vacuoles whose trafficking dynamics have been monitored (Cheng & Reese, 1987; Dailey & Bridgman, 1993). While attempting to elicit mechanosensitive currents from neurons (e.g., Morris & Horn, 1991), we used large osmotic excursions. A consistent event during neuronal shrinkage was uncontrolled vacuole formation, as if membrane trafficking had gone awry, producing out-sized endosomes. Here we use osmotic excursions to control the repeated appearance and disappearance of these structures: vacuole-like dilations (VLDs) large enough to be monitored by simple light microscopy and by confocal fluorescence microscopy. The responses of these VLDs under assorted swelling/shrinking conditions suggest that the underlying membrane dynamics are mechanosensitive. We postulate that the experimentally induced membrane behavior reflects a sensor/effector system strained to its limits by the stimuli. Normally, the system may allow neurites to detect local tension and effect appropriate surface area changes.

Methods

Cells and Solutions

Circumoesophageal ganglia were removed from mature *Lymnaea stagnalis* and placed into NS, an isotonic physiological solution ((mM) 50 NaCl, 1.6 KCl, 3.5 $CaCl_2$, 2.0 $MgCl_2$, 5.0 HEPES, 5.0 glucose; pH 7.6 adjusted with 1N NaOH; gentamicin added at 50 mg/100 ml; osmolarity 126 mosM), and gently agitated with 0.25% type XIV protease (Sigma, St. Louis, MO) in Ca-free NS for 30 min. After digestion, the ganglia were washed with NS. For plating in NS, one ganglion was placed in each Falcon 35 mm culture dish and teased apart with forceps, thus releasing neurons which settled and adhered to the dish. For the confocal microscopy images, cells were grown instead, on untreated glass coverslips. Experiments were carried out at room temperature (~20°C) 24–72 hr after plating.

The culture procedure yields a heterogeneous population of unidentified neurons (*see* Sigurdson & Morris, 1989) which adhere well with no substrates or growth factors provided. The neurons had a broad range of morphologies, from heavily arborized, through fried egglike to round with little evident peripheral lamella. Arborized cells were chiefly used in these experiments; exceptions are noted.

Deionized double distilled water was used wherever there is a reference to distilled water. The osmolarity of all solutions was measured with the Advanced MicroOsmometer (model 3MO).

Solution exchanges were made by hand using Pasteur pipettes; NS was drawn from the culture dish until only a thin film remained then replaced gently with experimental fluid. This exchange was done two more times for each plate. The entire procedure was completed in <30 sec. Aliquots taken from near the bottom of the dish were 2.5 ± 2.0 (SD, $n = 9$) mosmol at the end of the procedure (exchanging normal saline for distilled water). Solutions were made hyperosmotic by the addition of sucrose and hyposmotic by dilution with double distilled water.

The drugs, *N*-ethylmaleimide, cytochalasin B, nocadazole, brefeldin A, plus dimethylsulphoxide (DMSO) were all obtained from Sigma (St. Louis, MO).

Viewing Cells

An Olympus IMT-2 microscope fitted with Hoffman modulation contrast optics (objectives 10×, 20×, 40×) was used. Video recordings were made using a Sony CCD video camera (AVC-D5), JVC S-Xg super VHS cassettes and a JVC BR-S601 MU super VHS or a time lapse JVC BR-905 OU recorder. Video images, made with a Sony UP-850 video graphics printer and acetate tracings from a Hitachi video monitor were both used for measurements. For hard-copy video images, the brightness and contrast adjustments on the video printer were optimized. Some images were also processed through an Argus 50 contrast enhancer plus a Hamamatsu image processer for background subtraction. An out-of-focus image was not made during each experiment; instead, generic out-of-focus fields were videoed and used for background subtraction.

Labeling of VLDs with Aqueous Fluorescent Dyes

The labeling of neurons following osmotic perturbation was examined using fluorescent dyes, Lucifer Yellow (LY) or rhodamine-dextran 3000 (RD3000; Molecular Probes, Oregon) and confocal microscopy. To optimize the fluorescent signals neurons were cultured on glass bottomed culture dishes. VLDs formed as easily under these conditions as on plastic, but were smaller. LY in distilled water (100 μM) was added to the bath prior to the first media change and this concentration was thereafter maintained in all the rinsing solutions unless noted. Similarly, RD3000 (final concentration 25 μM) was also added to the culture prior to the osmotic perturbation and maintained throughout subsequent media changes. In the presence of either dye, neurons were not visible using conventional epifluorescence microscopy due to the intense signal from the out of focus fluorescence. In contrast, in the confocal microscope, the out-of-focus fluorescence was eliminated and the neurons were readily visible as black objects against a bright yellow (LY) or red (RD3000) background. In most cases neurons were also monitored with phase optics throughout the experiment.

Confocal Microscopy

Neurons were viewed with an inverted scanning confocal microscope (Bio-Rad MRC-600) equipped with an argon-ion laser (Mills, Neisen & Kerr, 1994; Mills et al., 1994), using fluorescein or rhodamine filter blocks and with a fluor (20×) or planapo (60×) objective. Emitted fluorescence was displayed through the framestore of the host computer. An adjustable pinhole in the detector lightpath controlled the optional section thickness and illumination intensity was controlled by the use of a filter wheel. A neutral density filter of 3 was used on all preparations. To visualize neurons in the presence of LY, the fluorescein filter set was used and for RD3000, the rhodamine filter block.

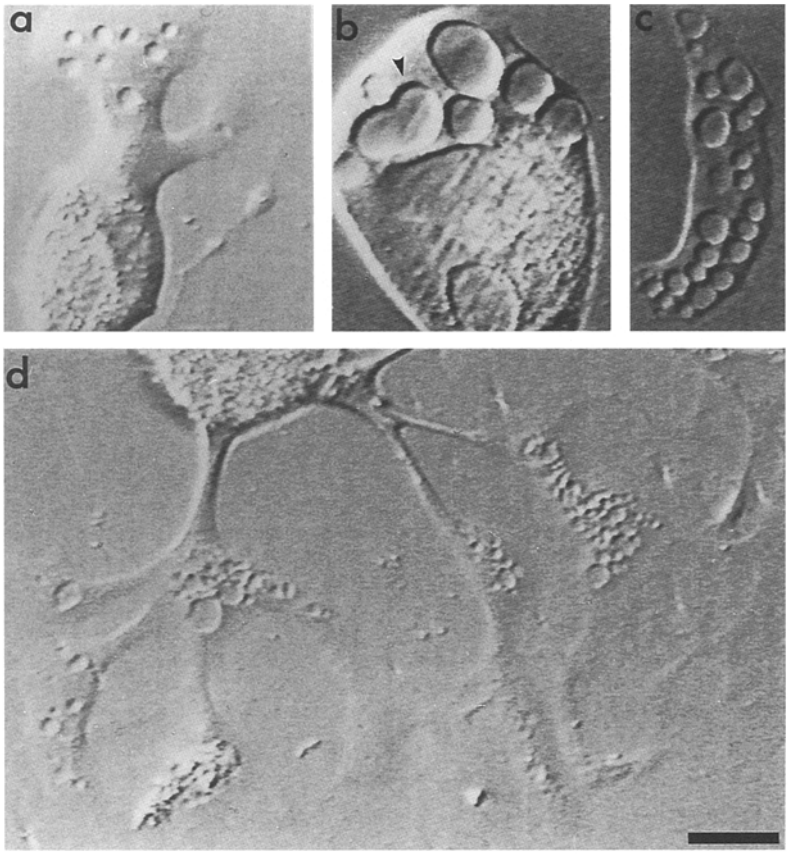

Fig. 1. Observation of VLDs. VLDs in growth cones and lamellae (*a, c, d*), at the base of unarborized cell (*b*) as well as adhesion sites along neurites where outgrowth is beginning (*d*). VLDs could form in isolated growth cones (*c*). Arrowhead in (*b*) indicates a pair of fusing VLDs. The VLDs appeared in NS following standard osmotic perturbations. Scale bar: 20 μm, *a* and *c;* 40 μm, *b* and *d.*

To follow the appearance of the VLDs, single confocal images were collected every 5–60 sec (but usually 10–15 sec) after osmotic shock. In some cases, simultaneous phase contrast images of the cells were also collected using the second confocal channel. VLD formation was also monitored by optically sectioning neurons; in this case optical series were taken using a single scan per section and step sizes (the distance between two optical sections) of 1–3 μm.

Results

Membranous Structures are Elicited by Osmotic Upshock

We subjected snail neurons to a wide range of osmotic upshocks and downshocks (increases and decreases in osmotic pressure, respectively). The term upshock and downshock are used because they describe the direction of an osmotic transition rather than absolute osmotic pressure. In our experiments, a standard osmotic perturbation or pulse constituted a downshock to distilled water (DW) for 2–4 min then an upshock to normal saline (NS). Upshocks cause shrinkage, downshocks cause swelling. Below, we describe how upshocks produced vacuole-like dilations (VLDs)—clear, reverse shadow-cast membrane-bound structures in the cytoplasm. Cultured *Lymnaea* neurons can withstand DW for >1 hr, whereafter, if returned to NS they can recover and reborize (Wan et al., 1994). Brief DW pulses were convenient because they triggered VLDs in 100% of the heterogeneous population *Lymnaea* neurons. Furthermore, a "short sharp shock" of DW was preferable as a standard perturbation because complex responses ensured during prolonged milder hypo-osmotic exposures. For example, left chronically in 0.3× NS, some neurons transiently formed small VLDs (they appeared at ~10 min and persisted until ~25 min).

VLDs induced by standard perturbations (Fig. 1) appeared and grew not after downshock when cells were swelling, but shortly after the upshock when cells were shrinking. Extensive swelling of vacuoles during a shrinking stimulus seemed counterintuitive, so a simple test was done to determine if fully formed VLDs were more than blisters under the cell or pits at the surface. Growth cone upper membranes were ruptured with a micromanipulator-mounted pipette. The flattened VLDs thus exposed assumed a spherical shape and behaved like loosely tethered membranous balls which could be dislodged intact. VLDs could also be manipulated inside intact growth cones. Gentle nudging made them slide partially over each other, firmer nudging dislodged them as membrane-bound compartments inside the cytoplasm where they could be further pushed around. Thus, while some VLDs may have been blisterlike, the microprobing

indicated that others were either (a) true vacuoles or (b) saclike invaginations constricted near the substrate and able to pinch off to become a vacuole. Below, we explore VLD topology further using extracellular dyes and find a continuum from blister, through deep invagination, to true vacuole.

As Fig. 1 illustrates, VLDs formed in growth cones, in broad lamellae (Fig. 1*a* and *d*), at the base of neurons (Fig. 1*B*). Along neurites, VLDs were evident only where incipient branches produced spreading adhesions. It was clear from focusing through the somata of unarborized neurons (Fig. 1*b*) that VLDs were situated near the substrate, not at upper or lateral surfaces. Given the principles of Hoffman optics (Hoffman, 1977) and assuming that the refractive index of cytoplasm exceeds those of saline and VLD contents, the images seen while focusing through growth cones indicated that large VLDs were like squashed hemispheres, rounded side up.

VLDs enlarged to diameters in the 10 μm range, often abutting each other (Fig. 1*c*) then coalescing as they pushed against each other (e.g., Fig. 1*b*).

VLD formation is not peculiar to *Lymnaea* neurons. Cultured bag cells (identified *Aplysia* neurons) exhibited the same response (*not shown*). Bag cells did not tolerate DW, but 2 min downshocks in 0.1× *Aplysia* saline (8-fold more concentrated than *Lymnaea* NS) yielded VLDs in growth cones upon upshock to normal *Aplysia* saline. Thus, VLDs formed in neurons of both freshwater and marine molluscs. Cultured rat hippocampal neurons and glia as well as cultured rat dorsal root ganglion neurons exposed to several minutes of ~0.7× or to 0.5× normal medium also exhibited VLDs upon return to normal medium (L.R. Mills and C.E. Morris, *unpublished observation*).

VLD Characteristics: Growth Rate and Amount of Membrane

Following a standard perturbation, VLDs appeared in *Lymnaea* neurons after a latency of <1 min then grew over the next minute to near-maximum size. Fig. 2 plots VLD diameter from the time at which they first became visible until growth ceased or VLDs coalesced. Since diameter changes of larger VLDs were easier to measure, the VLD diameter (~12 μm) at the plateau of the growth curve may overestimate the mean. VLDs became visible only ~0.5 min after completion of the upshock solution changes; increased optical resolution would be needed to determine if VLDs enlarged from pre-existing structures <0.5 μm diameter. Videographs of growing VLDs are shown in the Fig. 2 inset. Some VLDs had the form of blurry toruses as they first became visible but most VLDs first appeared as indistinct spots. For a VLD to grow from a submicroscopic sac of diameter, say 0.5 μm, to a 10 μm VLD would require a minimum of 157 μm^2 of membrane (assuming a VLD membrane area $\geq 2\pi r^2$).

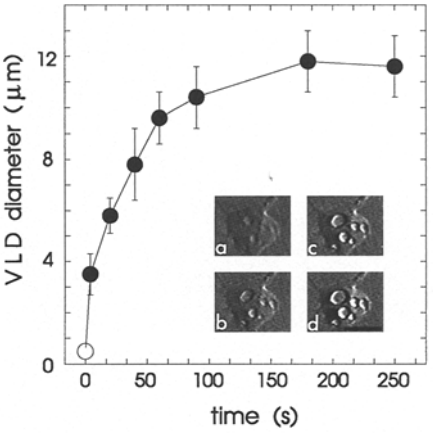

Fig. 2. VLD growth from first appearance until full size. Time = 0 is defined as the first visible indication of a structure that eventually resolved as a VLD. VLDs from six neurons (4–6 adjacent VLDs/cell) were measured; data points (filled circles) show SE for each cell (n = 6). Time = 0 began 15–35 sec after transfer from DW to NS; the open symbol is not a datum, but is positioned to indicate that previsible VLD structures would have had a diameter less than ~500 nm. Videomicrographs are from one of the cells at times 20, 50, 70 and 140 sec. Scale: 20 μm.

How VLDs grow is unknown but were vesicles involved, >2200 (150 nm diameter) would need to fuse for such a 10 μm VLD.

Mechanical, Not Chemical Perturbation Triggers VLD Formation

Osmotic perturbations using downshocks much milder than DW also triggered VLDs. VLDs formed in NS following 2 min pulses in 0.6×, 0.5× and 0.4× NS as well as 0.02× NS (0.02× NS = "DW"; *see* Materials and Methods). This indicates that the trigger in the standard perturbation was not exposure to "zero levels" of specific extracellular ions (e.g., Ca^{2+}, Na^{+}, Cl^{-}). Do mechanical (shrinkage) or chemical (concentration change) effects of the perturbations trigger VLD formation? The following results implicate mechanical rather than chemical factors.

When the DW in a standard pulse was substituted with a zero-ion isosmotic sucrose solution, VLDs did not form upon return to NS. Likewise, in experiments in which sucrose concentration was varied while tonicity was held constant during downshock (to 0.5× NS) and upshock perturbations, VLDs formed following the upshock. These results indicate that ion depletion associated with downshock was irrelevant to VLD formation.

As shown in Fig. 3, VLDs could be elicited by upshock from NS to 3.5× NS (425 mOsm). Under these conditions VLDs formed rapidly, though they occurred in a smaller proportion of cells— ~25%, not 100%— than after standard perturbations. By comparison with upshock-from-DW VLDs, these upshock-from-NS

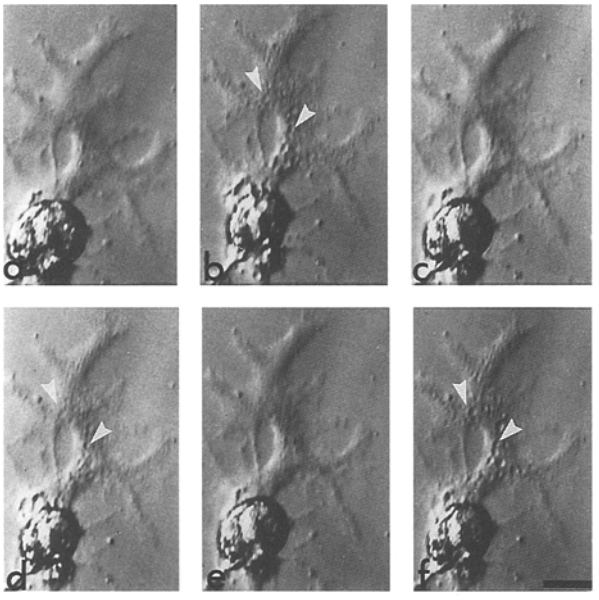

Fig. 3. Events following upshock from NS. Neuron in NS (*a*), was repeatedly given 2 min upshocks to 3.5× NS (*b, d, f*), with intervening 2 min downshocks to NS (*c, e*). VLDs appeared in the 3.5× NS and reversed on return to NS; arrowheads follow particular VLD sec. Scale: 20 μm.

VLDs were more common around the soma than in growth cones, they formed more rapidly, and remained smaller (5–6 μm diameter).

Taken together, these results from upshocks over a wide range of conditions suggest that VLDs were mechanically, not chemically induced. Upshock *to* NS and upshock *from* NS operate in the same direction mechanically (shrinkage, increased crowding of cytoplasmic structures, decreased tension in the membrane and adjoining structures). Chemically, however, the picture is different: upshock *to* NS renormalizes cytoplasm concentrations, whereas upshock *from* NS takes cell constituents from normal to abnormal. Since upshocks of both type (as well as upshock with no external ionic perturbation) triggered VLDs, whereas no VLDs formed if extracellular ions were removed without an osmotic perturbation, VLDs are not likely to depend on concentrations of particular solutes. Mechanical factors seem to be implicated. Moreover, the mechanical factors are evidently local to the VLD-forming part of the cell since VLDs formed as readily in isolated growth cones (Fig. 1*c*) as in intact neurons. In isolated growth cones, there is no opportunity for tension to be generated along a neurite or from the perikaryon.

Recovery Following VLD Formation—an Active Cellular Process

Large vacuolar structures, rare in newly isolated neurons in culture but common in aged neuronal cultures (Fig. 4*A*), are the tissue culture equivalent of the neuropathologist's "non-specific spongiform degeneration." We wondered if experimentally induced VLDs are features of terminally damaged cells, indicators of trauma following gross physiological insult, or alternately, an exaggerated display of normal cellular responses.

To assess this, we followed the fate of neurons in NS after VLD formation and found that individual and coalesced VLD membrane was reprocessed by the cell and that VLDs disappeared in 0.5 to 3 hr, depending on the extent of DW exposure. After a single 2 min DW pulse, full recovery required ~0.5 hr, whereas after longer or multiple perturbations, recovery took up to 3 hr. Thus, VLDs were transitory, not "terminal" cell features: the neurons recovered (e.g., Fig. 4*B*).

Viewed by time lapse, recovery coincided with a period of intense motor activity in the cytoplasm, a churning turmoil distinctly unlike Browninan organelle movements in cells traumatized by Ca^{2+} leak. When large fused VLDs formed (Fig. 4*C*), turmoil was especially dramatic. In time lapse, the turmoil had the appearance of continual kneading, pushing, constricting and severing of VLDs to smaller vacuoles. Refusion of newly severed VLDs sometimes occurred. During recovery, most VLDs shrank, retaining their distinct reverse shadowcast outline until they disappeared, some faded and shrank, and some faded to invisibility without changing diameter. Both extremes could be seen in the same neuron (Fig. 4*B*). Disappearance occurred in place; movement of a VLD away from its formation site as in Fig. 4*E* was evidently possible but was a rare exception.

Discrete Sites: VLD Formation is Reversible and Repeatable

In Fig. 5*A*, in DW after a downshock from NS, VLDs are seen shrinking and fading to invisibility. The sequence in Fig. 5*B* demonstrates that, in spite of the absence of visible foci (Fig. 5*Ba, b*), VLD initiation occurred not at random but at special sites. With repeated standard perturbations, VLDs formed repeatedly at the same locations on each upshock to NS (Fig. 5*Bc, e, g, i*). At each downshock to DW, the VLDs disappeared within ~1 min (Fig. 5*Bd, f, h*), but reappeared in NS. In these cycles, we use the term "reversal" for the rapid downshock-induced VLD disappearance. Note that this is distinct from "recovery" (Fig. 6). Reversal was a primary response occurring in the downshock medium and requiring ~1 min. Recovery occurred in upshock media, required at least several tens of minutes and was preceded by the primary upshock-induced effect, VLD formation.

Reversible, repeatable VLD formation at discrete sites also occurred when the osmotic perturbation in-

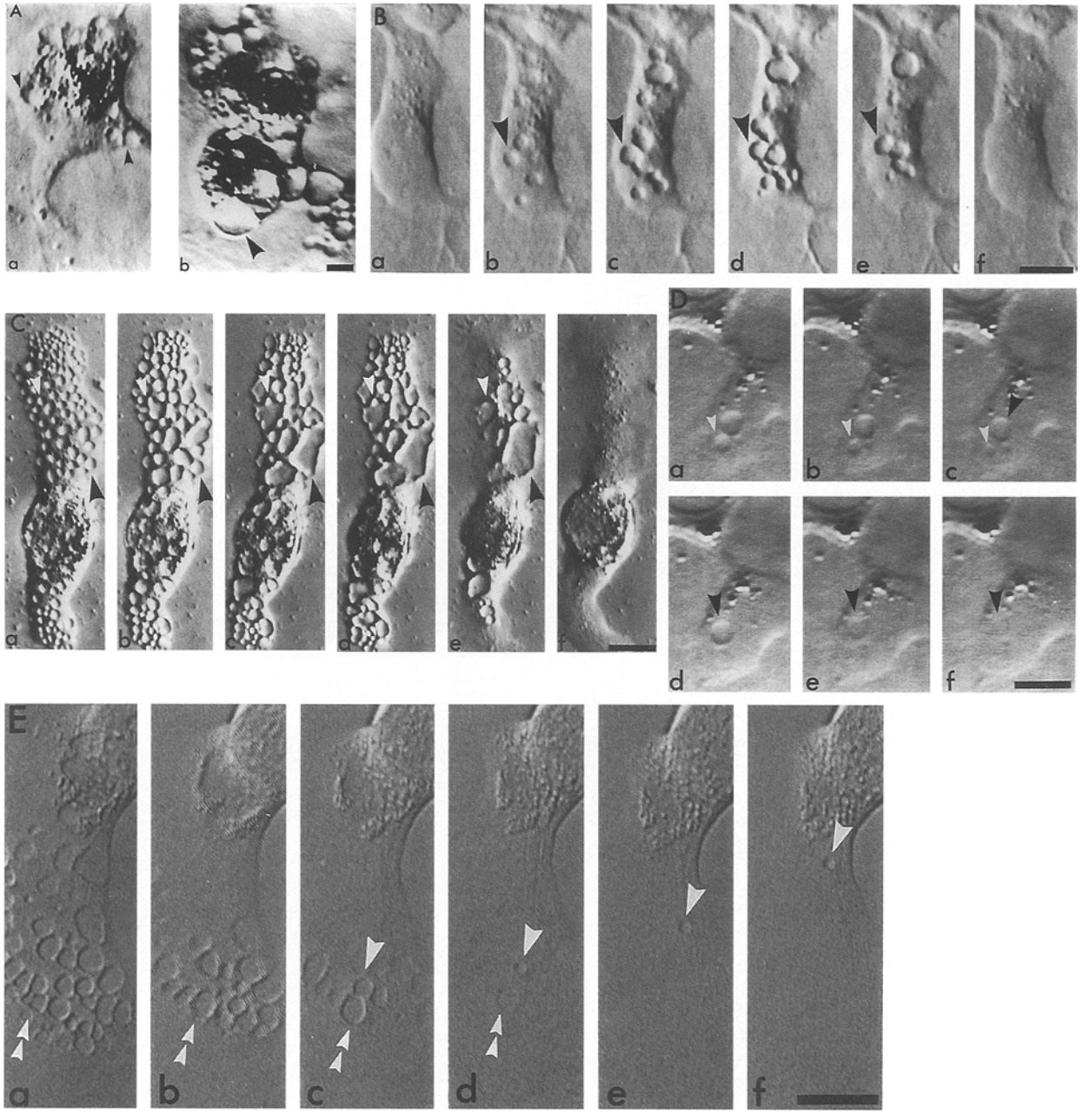

Fig. 4. Transience of the experimentally-induced VLDs: recovery. (*A*) Two examples (*a, b*) of vacuoles (arrowheads) that had formed spontaneously in degenerating neurons in an old culture (7 days). (*B*) Time series showing VLD formation and recovery after a standard perturbation; *a–f* show the neuron at 1.3, 5.0, 8.3, 14.3, 20.3, and 29.3 min after return to NS. Arrowheads indicate a specific VLD over this period. (*C*) Series emphasizing the coalescence of vacuoles during recovery: *a–f* show the neuron at 5, 15, 30, 40, 90, and 135 min after return to NS. The white and black arrowheads indicate VLDs that fused during recovery. (*D*) Disappearance modes during recovery. *a–f*, a recovering neuron at 12, 16, 20, 27, 30, and 35 min after return to NS. White and black arrowheads indicate VLDs disappearing by shrinking and fading respectively. (*E*) Unusual retrograde movement of a VLD following a standard perturbation. *a–f* show recovery at 20, 62, 95, 165, 185, 210 min after return to NS. Most VLDs disappeared in place, exhibiting a combination of fusion, shrinking and fading (e.g., double arrowhead), but one VLD (single arrowhead) moved retrogradely toward the cell body. Scale bars: 10 μm for A, 20 μm for *B–E*.

volved upshock-from-NS/downshock-to-NS (Fig. 3). On osmotically "naive" cells (i.e., no previous perturbation), a substantial upshock from NS was required to elicit VLDs; upshock to 3.5× NS was effective but upshock to 1.7× NS was not.

Discrete Sites Persist Even When Recovery Appears Complete

Particular ultrastructural configurations presumably underlie VLD initiating sites—configurations that might be

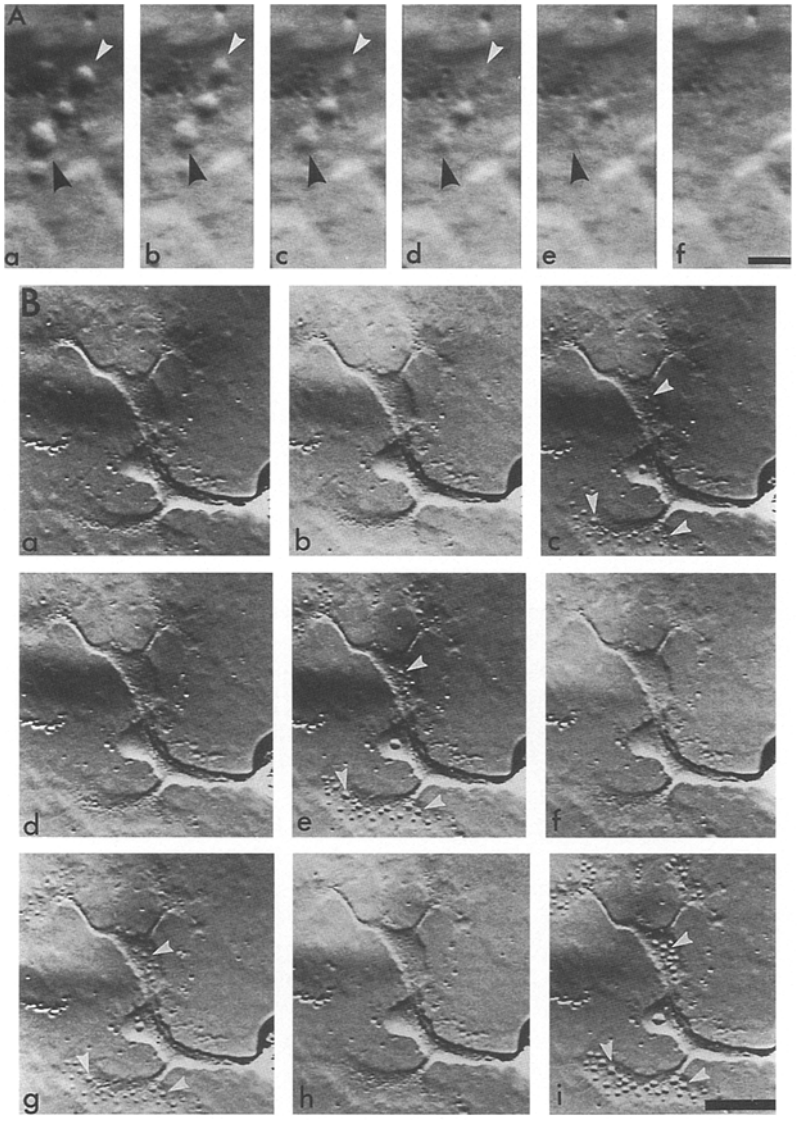

Fig. 5. Reversibility and repeatability of VLDs at discrete sites. (*A*) Reversal: time course of VLD disappearance in DW. After a standard pulse to a naïve cell, VLDs formed during 3 min in NS, then NS was replaced with DW: *a–f*, neuron in DW at 0, 1, 2, 3, 4 and 5 min. Black and white arrowheads indicate shrinking VLDs. Scale: 10 μm. (*B*) Four VLD formation/reversal cycles. (*a*) neuron in NS, (*b*) downshock to DW at 1 min, (*c*) upshock to NS 1 min later, (*d*) downshock to DW 1 min later, (*e*) upshock to NS 1 min later, (*f*) downshock to DW 1 min later, (*g*) upshock to NS 1 min later, (*h*) downshock to DW 1 min later, (*i*) upshock to NS 1 min later. Total time between *b* and *i*, 8 min. Arrowheads (*c, e, g, i*) indicate specific VLDs enlarging and shrinking at discrete sites. Scale: 20 μm.

dismantled in the cytoplasmic turmoil of recovery. To test whether VLD-initiating sites persisted throughout and beyond recovery, we gave neurons a standard perturbation, waited until VLDs formed and recovery was underway, then gave a further perturbation. Recovery was considered to have begun when VLD growth ceased (turmoil was evident by this point) and to be complete when no visible VLD remnants remains. Once recovery began, an interval of 5, 10, 30 or 120 min was allowed to elapse before the next standard perturbation. Four dishes were tested; in each, an individual neuron was monitored continuously, receiving 2 or 3 standard perturbations after the initial one. The final one (always after a 120 min interval) was on fully recovered neurons. Outgrowth during these runs was negligible.

Two results were noted. First, with recovery underway (i.e., at 5-, 10- or 30-min intervals), any still-visible VLDs reversed in response to downshock to DW. Second, for all intervals (5, 10, 30 and most importantly, 120 min), upshock to NS elicited VLDs at previous sites. Thus VLD sites persisted throughout 120 min of recovery, outlasting the VLDs themselves.

The existence of persistent sites was further manifested in trials using upshock from NS. As indicated above, upshock to 1.7× NS elicited no VLDs in osmotically naive cells. However, in neurons recently recovered from a standard perturbation, upshock from NS to 1.7× NS elicited in 100% of neurons, VLDs at the sites where they had first appeared. They then reversed within minutes of downshock to NS. The fact that a normally ineffective upshock became profoundly VLD-inducive after VLDs had been made once confirms that

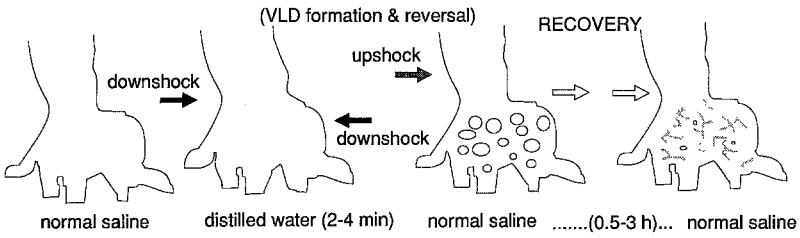

Fig. 6. Schematic of a growth cone undergoing a standard perturbation and illustrating two types of VLD disappearance: reversal and recovery. A naïve neuron, on the left, is submitted to a standard perturbation (2–4 min DW then back to NS). VLD formation ensures with the upshock. VLDs reversal occurs if the neuron is again given a downshock. The neuron can be repeatedly cycled through upshock and downshock, with, as in Fig. 5, repeated formation and reversal of VLDs. Recovery ensues after an upshock if the neuron is left in NS. Turmoil in the cytoplasm adjacent to VLDs in the recovering neuron is indicated graphically.

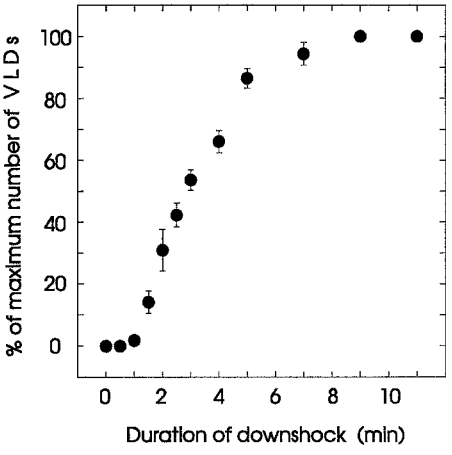

Fig. 7. The number of VLD sites/cell. The % of the maximum number of VLDs/cell is plotted as a function of the duration of the DW pulse used to elicit VLDs. Twenty cells were given at least three different DW pulses. The maximum number of VLDs/cell (determined following DW pulses ≥5 min) ranged from 20–79. Cells underwent recovery between pulses; pulse sequence (in terms of duration) was random. Some cells did not withstand DW pulses >4–5 min; these were not included. Infrequently, neurons were noted whose lamellae formed hundreds of just-visible VLDs at the outer rim (*not shown*); such cells were excluded.

even though recovery appeared complete some of the changes had not been redressed. On a separate issue, these trials also support the idea that VLD reversal is mechanically driven. VLD *reversal* induced by downshock-to-NS and eventual *recovery* after upshock-to-NS both occurred in NS. Thus, the mode of VLD disappearance does not depend on the absolute osmolarity of the solution; rather, the disappearance is a reversal (fast mechanical response to swelling) if the transition to NS constitutes a downshock and a recovery if the transition to NS constitutes an upshock.

The Number of Sites for VLD Formation Saturates

If discrete sites reflect specific, albeit unresolvable VLD-initiating structures, VLD numbers should saturate at large stimuli. Fig. 7 shows that, indeed, VLD numbers depended sigmoidally on the duration of the downshock perturbation. DW pulses <1 min triggered no VLDs, ~2–7 min pulses recruited VLDs in increasing numbers, and longer pulses recruited no more. Hydrostatic pressure does not change instantaneously following an osmotic step; rather the perturbations' mechanical impact (e.g., tension in membranous and cytoskeletal structures) is a time integral. Accordingly, DW pulses <1 min were subthreshold for VLD formation (Fig. 7). As implied earlier, a threshold was also noted for stimulus amplitude; a 2 min 0.7× NS pulse was subliminal, 0.6× NS produced VLDs in some cells, 0.3× NS in most cells, and 0.02× NS, universally. Fig. 7 is, in essence, a dose-response curve in which the x-axis reflects the concerted extent (''dose'') of tension excursions. Saturation was not a foregone conclusion; larger stimuli might have initiated increasingly smaller numbers of bigger VLDs or increasingly greater numbers of smaller VLDs rather than revealing a fixed number of initiating sites as indicated by the sigmoid curve.

VLD Formation and Reversal are Not Dependent on Extracellular Ca^{2+}

In neuronal somata, swelling and shrinking increase and decrease the electrically detectable quantity of plasma membrane, independent of extracellular Ca^{2+} (Wan et al., 1995). We tested whether VLDs depended on extracellular Ca^{2+} in order to determine if conventional exocytosis (and hence Ca^{2+} influx) was required for VLD dynamics.

Repeated VLD formation/reversal cycles could be elicited with sub-μmolar extracellular Ca^{2+} during otherwise standard perturbations (low-Ca^{2+} saline: NS except 0.5 mM Ca^{2+}, 1 mM EGTA, giving free [Ca^{2+}] 0.5 μM). Moreover, when these perturbations were repeated, VLDs formed repeatedly at the same sites in low-Ca^{2+} (Fig. 8). (Zero-Ca^{2+} NS was impracticable because the cells lifted during solution changes.)

There was no evidence of a subpopulation of Ca^{2+}-dependent VLD sites. Experiments were done with two

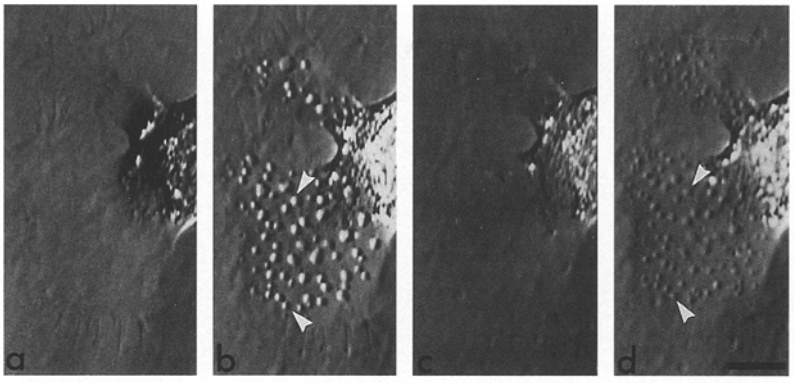

Fig. 8. VLD formation and reversal was not dependent of the extracellular Ca^{2+}. Neuron in NS was treated for 15 min in low-Ca^{2+} NS and then given first one low-Ca^{2+} standard perturbation (DW plus 1 mM EGTA (*a*), upshock to low-Ca NS (*b*)), then another (*c, d*). VLDs formed upon upshock to low-Ca^{2+} NS (*b, d*) at the same sites (arrows). Scale: 20 μm.

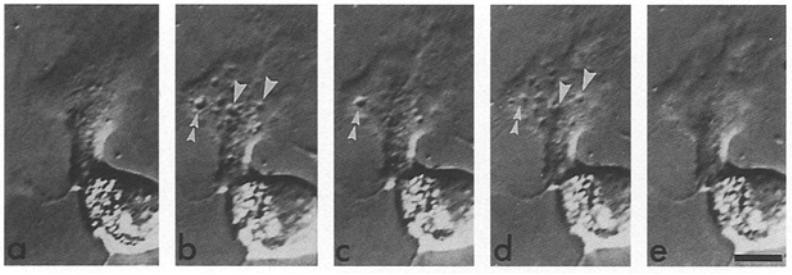

Fig. 9. Effects of cytochalasin. After 30 min in NS with 40 μM cytochalasin B, a neuron was subjected to repeated standard perturbations with cytochalasin/DMSO present throughout. (*a*) DW, (*b*) NS, (*c*) in DW when reversal is only partway complete (double arrowheads point to a VLD that has not yet reversed), (*d*) NS, (*e*) DW. The repeated upshocks (*b,d*) led to VLDs at the same sites (single arrowheads). Scale, *a–e:* 20 μm.

or three standard perturbations, then a low-Ca^{2+} one. This last perturbation yielded VLDs at all sites noted previously with Ca^{2+} available.

Thus, reorganization of membrane during VLD dynamics required no Ca^{2+} influx across the plasma membrane; how *intracellular* Ca^{2+} behaves during VLD dynamics remains to be determined.

Recovery was impaired by low-Ca^{2+}. Although cells left in low-Ca^{2+} NS after VLD formation exhibited some of the membrane and cytoplasmic activity associated with recovery in normal NS, recovery was invariably incomplete at 3 hr (Table).

Differential Effects of Cytochalasin B on Reversal and Recovery

During recovery, turmoil around the VLDs indicated that motor proteins were highly active. In molluscan neurons (Kutznetsov et al., 1992) membranous organelles are actively moved along actin filaments. To test for involvement of the neurons' pool of dynamic (actively polymerizing, depolymerizing) actin in VLD dynamics, we used cytochalasin B, an agent which promotes depolymerization of filamentous actin (Table, Fig. 9). Cells were pretreated for 15–30 min with 10 or 40 μM cytochalasin B in 0.5% DMSO, subjected to standard perturbation, the returned to NS with the cytochalasin/DMSO. In cytochalasin/DMSO controls given no osmotic perturbation, the drug caused some VLD formation. The overall cytochalasin-induced "VLD-background" was <10% of VLDs produced by a standard perturbation, but the background was highly nonuniform. Whereas most cells showed no VLDs or only one or two, ~5% of neurons were as VLD-laden as if they had received a standard perturbation. The "background VLDs" are probably comparable to "macrovacuoles" induced by cytochalasin in fibroblasts (Brett & Godman, 1984).

Standard perturbations caused cytochalasin B treated neurons to produce VLDs as rapidly and as extensively (100% of cells) as in untreated cells. Up to the point when VLDs attained full size, cytochalasin B had no discernible effect on VLD dynamics, but adjacent VLDs never coalesced. The abolition of coalescence by cytochalasin may simply mean VLD-VLD fusion normally occurred when contractile turmoil happened to push VLDs together.

VLD reversal, like VLD formation, was unaffected by cytochalasin B treatment (Fig. 9*c, e*). Moreover, when cytochalasin-treated cells were given multiple perturbations (as in Fig. 5), they showed cycles of VLD appearance and reversal at discrete sites (Fig. 9*b, d*) just as in untreated cells.

"Background VLDs" (i.e., from cytochalasin/DMSO treatment alone) were reversed by a downshock to DW. At a subsequent upshock, VLDs reappeared (in their initial positions), along with a full crop of osmomechanically induced VLDs (DW pulses caused VLDs to form in all cells). Thus, regardless of whether a DW pulse or cytochalasin originally induced them, VLDs responded identically to downshock and exhibited repeatability at discrete sites.

Recovery of VLDs in NS was completely blocked by cytochalasin B treatment; VLDs grew to full size but

Table. Effects on VLDs of various treatments which disrupt cellular organization

Treatment	VLD formation: blocked?	VLD reversal: blocked?	VLD recovery:	
			Disappearance blocked?	Turmoil blocked?
Cytochalasin B (10 or 40 μM in 0.5% DMSO)	No	No	Yes	Yes
N-ethylmaleimide (1 mM in NS)	No	No	Yes	Yes
Nocodazole (10 μM in 0.03% DMSO)	No	No	No	No
Brefeldin A (17.8 μM in 0.01% ethanol)	No	No	Yes	Impaired (movement normal but coalescence reduced)
0.5% DMSO control	No	No	Slowed	No
No extracellular Ca^{2+}	No	No	Slowed	Impaired (movement normal but coalescence reduced)

thereafter were static for 3 hr. The fact that the cytoplasmic turmoil and VLD disappearance were both abolished suggests that turmoil reflects motor activity requisite to the reprocessing of VLD membrane. The solubilizing agent, DMSO, had a minor effect. It slowed recovery; in DMSO alone, most cells showed VLD remnants at 3 hr.

N-ethylmaleimide, Brefeldin A and Nocodazole

Myosin bears the ATPase of the actomyosin motor. There are no specific myosin-inhibitory drugs, but *N*-ethylmaleimide (NEM) is a sulphydryl reagent which abolishes the ATPase activity of myosin (Lawson, 1987). Neurons in 1 mM NEM (pretreatments were as with cytochalasin B) responded to standard perturbations (Table) like neurons treated with cytochalasin. They were fully capable of repeated VLD formation/reversal cycles at discrete sites, but both aspects of recovery were blocked.

NEM is a difficult physiological tool. Among its many actions, it binds the NEM-sensitive fusion protein, NSF (Block et al., 1988), a cytoplasmic protein involved in the fusion of vesicles to target membranes. NEM's anti-actomyosin action is however, a good candidate for its abolition of recovery, since the contractile turmoil of recovery was absent, echoing the case when myosin's motor partner, actin, was incapacitated. Another indication that NEM inhibited motor proteins was the cessation of the filopodial movements normally evident in time-lapse recordings. NEM also abolished writhing of osmotically swollen neuronal somata (Wan et al., 1995).

Thus we conclude (a) that VLD formation and reversal required no actomyosin motor, and (b) (with less certainty because of NEM's nonspecificity) that recovery probably did. VLD formation and reversal were insensitive to NEM at the cytoplasmic levels achieved with 1 mM NEM in the bath, making it unlikely that NSF protein participates in these events though it may do so in recovery.

Brefeldin A disrupts golgi, but also interferes with postgolgi membrane trafficking (Reaves & Banting, 1992). We used it at a concentration (Table) shown to disrupt transport of a specific golgi protein between the golgi and plasma membrane. As with the other drugs, cells were pretreated, subjected to a DW pulse, then exposed again to the drug. Brefeldin A actions (Table) differed from those of cytochalasin B and NEM in a revealing way. VLD formation and reversal were unaffected. Recovery was blocked but the mechanism differed from that for cytochalasin and NEM. With brefeldin A, the cytoplasmic turmoil typical of controls was not blocked, yet reprocessing and disappearance of the VLDs did not occur. This difference is consistent with brefeldin A's known actions—it is a disrupter of membrane processing but is not known to act on motor proteins.

Nocodazole was used at 10 μM (Table). In rat sympathetic neurons, 6.6 μM nocodazole depolymerizes 50% of microtubules in 5 min (Baas & Black, 1990) and in *Aplysia* neurons, 2 μM profoundly disrupts the formation of microtubule based protrusions (Goldberg & Burmeister, 1992). As with the other drugs, the protocol involved a pretreatment, a standard DW perturbation, then further treatment. Nocodazole produced no discernible effects on VLD dynamics.

Confocal Microscopy

To determine the relationship between VLD contents and extracellular fluids, aqueous fluorescent markers were used in the bath.

Initially we tried epifluorescence, using Lucifer Yellow (LY) as an extracellular marker. During a standard perturbation with LY in the bath (NS/LY—DW/LY—NS/LY), VLD formation was monitored by phase contrast, then minutes later, when repeated washes in LY-free NS had cleared LY from the bath, cells were visualized by epifluorescence. Most VLDs were marker free, but a small fraction were fluorescent. Subsequent downshock reversed all VLDs (as monitored by phase contrast); the fluorescent ones lost their LY during reversal. This suggested that bath fluid entered growing VLDs, but that the entry point was mechanically labile, becoming constricted to a variable degree. On transfer to LY-free NS, fluorescence washed out of most VLDs (most therefore, must still have been patent) but was retained in a small fraction (this fraction was, therefore, fully constricted) until a subsequent downshock reopened the access route.

The trials with epifluorescence pointed to the need for continuous monitoring of the bath marker during VLD formation and reversal. We have made preliminary confocal microscopy observations using LY (not shown) and rhodamine-dextran 3000 (RD3000) (Fig. 10); they indicate that confocal fluorescence imaging can be used to simultaneously image bath and VLDs. As Fig. 10 shows, in-focus bath fluorescence demarcated the plasma membrane/cytoplasm boundary, whereas out-of-focus bath fluorescence was not visible. We established the following points: (i) In controls (NS + RD3000), extracellular marker did not percolate into cytoplasmic regions, indicating that prior to a standard perturbation, no invaginations were open to the bath. (ii) Likewise, during downshock, cytoplasm did not take up marker. (iii) Following upshock, as VLDs (e.g., Fig. 10*iA*) formed, VLD contents were contiguous with the bath (e.g., Fig. 10*ii*). (iv) VLDs extended up from the substrate adhesion plane, creating blind-ended tunnels in the cytoplasm. They did not perforate the upper surface of the cell (Fig. 10*ii*). (v) No upshock-induced "fluorescent inlets" were seen at sites remote from the substrate. (vi) During a downshock (in the continued presence of bath tracer) VLD fluorescence shrank circumferentially during reversal till fluorescence and VLDs disappeared (Fig. 10*iA–F*). (vii) Very few VLDs retained fluorescence after NS washout of bath marker (*not shown*), hence most VLDs did not fully constrict during the course of the experiment. (viii) The spongy appearance of optical sections through cell adhesion planes during VLD formation (e.g., Fig. 10*iiA*) suggests that bath fluid percolated between adhesive contacts to enter VLDs.

Discussion

The results presented here show that *Lymnaea* neuron membranes are impressively robust and plastic (*see also* Wan et al., 1995). This may be common in neurons; squid axons stretched to double their length then released, generate large vesicles beneath the axolemma (Fishman et al., 1990). Mechanical robustness and compliance probably reflect mechanisms that control membrane disposition during neuronal outgrowth and retraction and during imposed stretch. If new surface membrane is rate-limiting during outgrowth, mechanical stimulation of membrane insertion would enhance outgrowth. This could explain why growth cones pull before they elongate (Lamoureux et al., 1989) and why hypo-osmolarity (50% normal) induces chick neuron outgrowth at ~6 times the control rate, while hyperosmotic medium reduces outgrowth (Bray et al., 1991; *see also* Heidemann, Lamoureux & Lin, 1994). Insofar as excessive tension rips membrane and insufficient tension leads to loss of cell shape, mechanical feedback is needed. Mechanosensitive ion channels in snail neurons are poor candidates for feedback transducers (Morris & Sigurdson, 1989; Morris & Horn, 1991; Small & Morris, 1994). Cell surface integrins may transmit mechanical signals to the cytoskeleton (Wang, Butler & Ingber, 1993) but no evidence yet links integrin-based mechanotransduction to the membrane insertion/retrieval.

"Retrieval Vacuoles" and "Insertion Disks" in Relation to VLDs

A bottleneck in membrane processing would occur if large areas of plasma membrane suddenly entered the retrieval-traffic stream. VLDs may represent such bottlenecks. They may start as membrane-attached endocytic vacuoles which acquire new membrane faster than the rate of vacuole breakdown (Fig. 11). A dynamic continuity between endosomes and plasma membrane is directly evident by enhanced-resolution DIC videomicroscopy of sympathetic neuron growth cones (Dailey & Bridgman, 1993) in which small reverse shadowcast vacuoles are normal participants in membrane trafficking. That the vacuole membrane derives from retrieved plasma membrane was shown by following identified vacuoles at the EM level, using ferritin. In optic tectum growth cones *in situ,* vacuoles flattened to lumenless disks constitute the dominant cytoplasmic membrane store (Cheng & Reese, 1987); tracer studies indicate that in growing neurites, the vacuoles are more commonly involved in insertion than in retrieval.

Thus, two-way traffic can be mediated by the endosomal membrane. VLDs in molluscan neurons may be extreme variants of these retrieval and insertion phenomena. Membrane machinery closely allied to synaptic

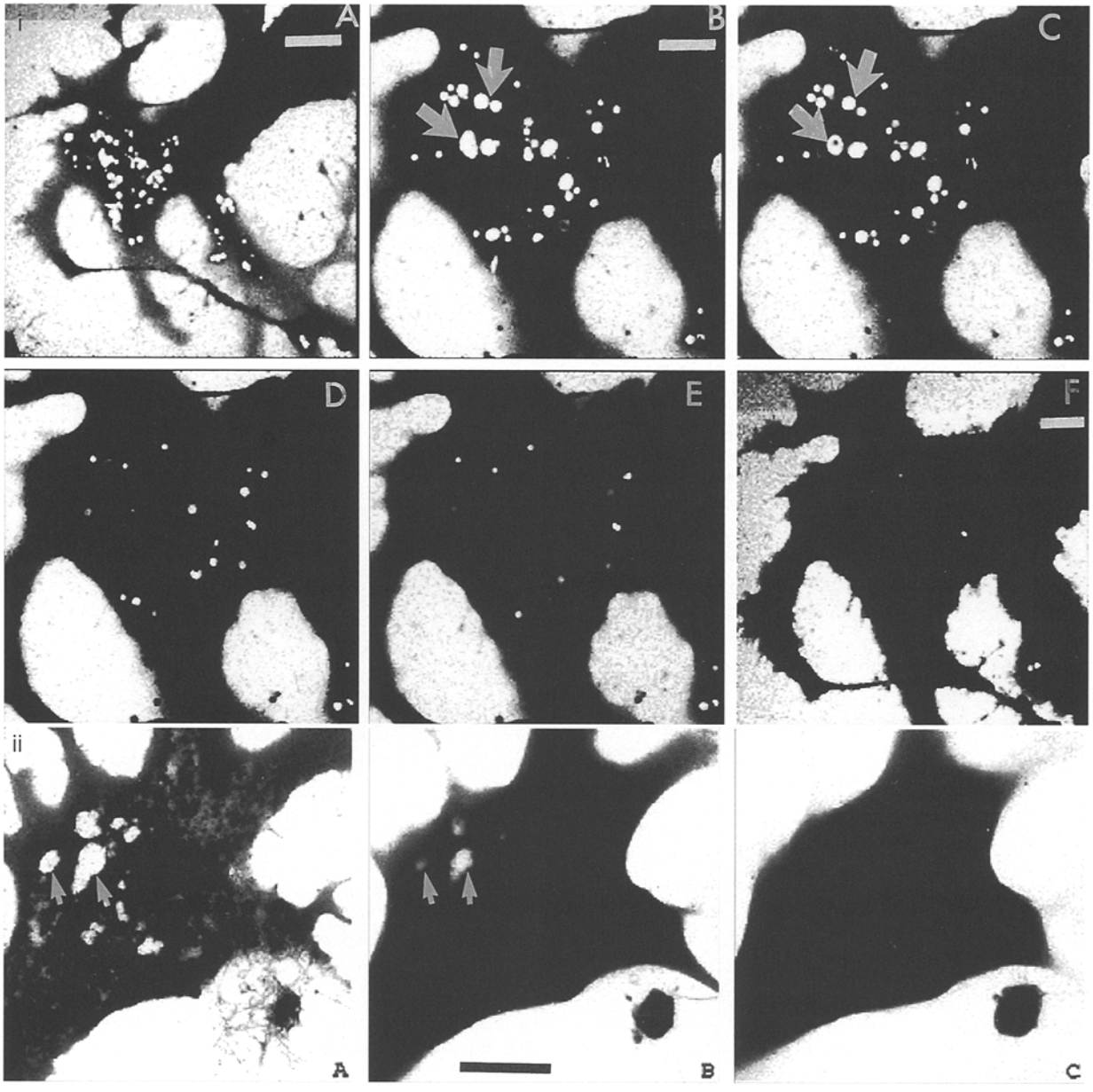

Fig. 10. VLDs viewed by confocal fluorescence microscopy of the extracellular marker, RD3000. (*i*) Time series showing VLDs in a veil area undergoing reversal in DW. *A–F* correspond to 0, 1.0, 1.3, 1.9, 2.2 and 2.3 min, respectively, all in the same plane, 3 μm up from the substrate. At time 0 (*A*), ~1 min after a standard perturbation that induced VLDs, the neuron was in NS/RD3000. Between (*A*) and (*B*), the bath solution was changed to DW/RD3000. Over a period of <1.3 min (i.e., from *B–F*), while the VLDs reversed, the fluorescent profiles disappeared. Scale bars: *A* 20 μm, *B–E* 12 μm, *F* 15 μm. (*ii*) Vertical series through cell body. (*A*) is at the substrate, (*B*) is 3 μm up and (*C*) is 6 μm up. In addition to VLDs (arrows), the cell/substrate contact plane (*A*) shows regions of reticulated fluorescence, suggesting that bath medium is drawn into VLDs by percolating under the cell. Similar reticulations, but no VLDs, were seen at the base of neurons that had not been osmotically perturbed. Reticulations were not seen at higher planes. *A–C* show how a vertical series conveys the approximate shape of VLDs. In this case, the VLDs evident in (*A*) tapered sharply, extending <6 μm up (*B, C*); these may be the type of VLDs that fade in Hoffman optics and that do not pinch off and become vacuoles. In other vertical series, VLDs were more tunnel-like and extended further (some >7.5 μm). *A–C* were taken as recovery was beginning; the cell had been in NS/RD3000 for ~8 min after a DW pulse. Scale bar, 22 μm.

endings—specialized endosomal/vesicular compartments—is evidently widely used to allow rapid transient modification of nonsynaptic cell surfaces (Kelly, 1993; Steinhardt, Bi & Alderton, 1994).

Relation to Phenomena in Other Cell Types

Membrane dynamics suggestive of two-way mechanosensitive membrane trafficking occurs in various cells. Bladder cells, for example, accommodate osmotically or

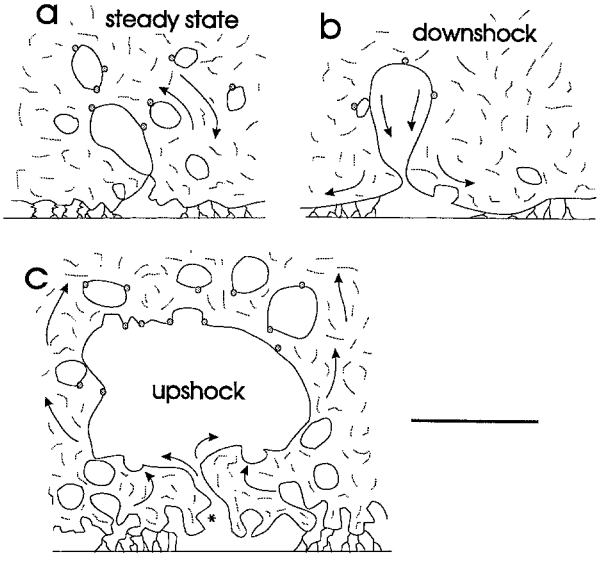

Fig. 11. Model for membrane rearrangements at VLD sites. *a, b* and *c* depict part of a region where a neuron has attachments to the substrate. The general scale is suggested by a bar for 0.5 μm, the microscopy resolution limit. Small nonadherent membrane patches regions adjacent to adhesions serve as foci for membrane traffic and can become VLD initiating sites. Extracellular rhodamine-dextran entered VLDs as they formed but did not otherwise percolate into juxtacytoplasmic regions. Accordingly, the VLD site is depicted as harboring a closed-off endosome in the steady state (*a*); fusion of endosomes is promoted by swelling stimuli (downshock) (*b*). During subsequent shrinkage, the non-adhering membrane area becomes the locus of an enlarging invagination. In other words, a VLD forms (*c*), becoming visible upon exceeding ~0.5 μm. In some cases, the neck of the invagination (asterisk) becomes fully constricted and the VLD pinches off as a true vacuole. Arrows indicate membrane dynamics: at steady state, membrane movement between surface and cytoplasm is balanced, during downshock net movement is toward the surface, and during upshock net movement is from the surface towards internal stores in the cytoplasm. Filamentous actin is required for recovery, so the VLD (and endosomes) are depicted as having unspecified machinery (attached circles) to allow for an interaction with actin. Actin has been shown to interact with synaptotagmin (Feany & Buckley, 1993) during endosome breakdown.

mechanically induced stretch by incorporating membrane from a cytoplasmic pool into the apical membrane (Lewis & de Moura, 1982). Release of stretch results in return of membrane to the cytoplasm on a 5 min time scale, a result that seems to echo reversible VLD formation in neurons. Rat liver cells swell when incubated at 10°C, then on rewarming, produce fluid-filled vacuoles whose formation is insensitive to cytochalasin B and colchicine (van Rossum et al., 1987). Fibroblast motility is integrally linked to membrane trafficking. Fibroblasts exposed to cytochalasin become immotile and develop discrete endoplasmic "macrovacuoles" derived from plasma membrane (Brett & Godman, 1984). In effect, plasma membrane, present in excess after tractile motility ceases, is internalized. Cytochalasin simultaneously blocks tractile forces and impedes the processing of the newly internalized membrane. The resulting bottleneck generates macrovacuoles which, upon removal of cytochalasin, are reprocessed into vesicles.

The vacuologenic protocols for fibroblast, hepatocyte and neuronal findings all fit a scheme consistent with Fig. 11: (*a*) vacuole formation is preceded by a relaxation of cellular tension. In the neurons, decreased tension results from upshock; in hepatocytes, decreased tension results when rewarming activates the ion pumps that counter cell swelling; in fibroblasts, decreased tension results when cytochalasin inhibits actomyosin-based tractile tension. (*b*) VLD formation in neurons, rewarming-induced vacuolation in hepatocytes and rounding-induced macrovacuole formation are all cytochalasin-insensitive. (*c*) in neurons, VLD recovery, and in fibroblasts, macrovacuole recovery was blocked by cytochalasin. (*d*) cytochalasin-induced vacuoles ("background VLDs") in *Lymnaea* neurons (analogous to cytochalasin-induced vacuoles of fibroblasts) behaved like VLDs: they reversed with a downshock then reappeared at the same site with an upshock.

A further parallel between neuron and fibroblast comes from electrorotation measurements (a noninvasive indicator of membrane area) of fibroblasts undergoing osmotic perturbations which led to the conclusion (Sukhorukov, Arnold & Zimmermann, 1993) that there exists an intracellular pool of "instantly available" membrane whose deployment is largely reversible.

Fig. 11 proposes a scheme for VLD formation, reversal and recovery in snail neurons. If "downshock and upshock" are read as "increased and decreased tension," the scheme becomes one for mechanosensitive membrane disposition. How membrane moves to and from the VLD during VLD formation (Fig. 11*c*) or reversal (Fig. 11*b*) is unknown, but the scheme suggests possibilities that could account for our observations. In steady state (Fig. 11*a*), near sites of anchorage to the substrate, endosomal vacuoles establish continuity with the plasma membrane at one of a finite number of sites (punctate areas of reduced adhesion seen by interference reflectance microscopy in vertebrate growth cones (Heidemann et al., 1994) might be coincident with VLD-initiating sites). Under swelling tension, the endosome fusion (Fig. 11*b*) and membrane outflow is promoted at the site. When tension falls, inflow predominates (Fig. 11*c*); it is envisaged that site constituents focus retrieval of vesicles and/or promote inward flow of plasma membrane. Note that actomyosin is not shown participating in mechanosensitive steps *per se* but in the reprocessing of large endosome/VLDs.

Mechanisms for Mechanosensitive Externalization and Retrieval

Swelling promotes both membrane externalization (Wan et al., 1995) and VLD reversal independent of Ca^{2+} in-

flux. Downshocks may elevate intracellular Ca^{2+} and hence promote exocytosis, or tension may directly promote vacuolar/plasma membrane fusion. Though stretch channels (Morris & Sigurdson, 1989) are not likely participants in mechanosensitive membrane fusion, they illustrate that tension can activate or inactivate selected membrane proteins. For already-attached endosomes or VLDs, externalization may be facilitated by simple pulling, as depicted in Fig. 11*b*. The simple fact that a taut membrane must "pucker" prior to being internalized might suffice to render constitutive internalization or retrieval mechanosensitive.

Fig. 11 can incorporate other facets of *Lymnaea* VLDs, namely: (i) that cytochalasin- and upshock-induced VLDs, once formed, were indistinguishable, (ii) that reversal was possible throughout recovery, cytoplasmic turmoil notwithstanding, (iii) that distinct VLD sites persisted for a short time after recovery appeared complete.

Wang et al. (1993) provided evidence for a tensegrity-based mechanotransduction system capable of essentially instantaneous signalling via interconnected cytoskeletal elements. VLD dynamics were unaffected by cytoskeleton agents, so it is unlikely that they depend on a tensegrity system for the cytoskeleton, but the tensegrity system and mechanosensitive membrane trafficking might operate smoothly in parallel, perhaps sharing tension information conveyed from points of adhesion.

Neurite outgrowth requires incorporation of membrane (Popov et al., 1993) and stalls if the growth cone produces no tension (Lamoureux et al., 1989); forces generated by motor proteins may control the insertion of appropriate amounts of membrane along the neurite. Outgrowth requires no Ca^{2+} influx (Campenot & Draker, 1989) nor did swelling-induced VLD reversal or swelling-induced capacitance increases (Wan et al., 1995). A tantalizing possibility is that VLD sites are normally used for pulling-induced insertion of membrane.

Mechanosensitive Membrane Disposition and Pathology

VLDs, we suggest, represent an experimentally induced pathology of a normal membrane addition/subtraction process. In a similar vein, upshocks associated with fixatives may sometimes induce vacuolation that is noted by pathologists. Our attempts to fix swollen neurons using aldehyde fixatives invariably triggered VLD-formation (*unpublished observation*), presumably because the fixatives were severely hyperosmotic. Vacuolation noted in cingulate neurons following administration of *N*-methyl-D-aspartate antagonists (Olney et al., 1991) is evidently not the pathological condition *per se*, but a fixation artefact (Auer & Coulter, 1994). Our findings suggest that the cingulate neurons may be preferentially vacuolated by fixation because systemically-applied antagonist makes them so hyperactive that the resulting energy deficit causes swelling. This makes them vulnerable to aldehyde fixative triggering of VLDs.

Some cells respond to diverse noxious stimuli (e.g., osmotic swelling, energy deprivation, hyperthermia, focally applied suction, exposure to cytochalasin) by extruding membrane blebs (Gabai & Kabakov, 1993; Hoffman, Jessen & Dunham, 1994; Milton & Caldwell, 1990). This raises the possibility that VLDs are internalized blebs. Though we did not observe blebs during swelling or cytochalasin treatment, it is possible that similar membrane pools contribute to at least some bleb types (e.g., the suction-induced blebs) and to VLDs. We have suggested that, during swelling, membrane moves from internal stores to the surface via sites that can initiate VLDs. During swelling, endosomes may fuse and their bilayer lipids may flow centripetally (as in Fig. 11*b*) from sites along a scaffolding of membrane skeleton that has expanded under the increased tension (e.g., Ursitti & Wade, 1993). Then, with subsequent cell shrinkage, the deceased membrane/membrane skeleton tension may favor a reverse flow (as in Fig. 11*c*) at the VLD site. In diverse vacuolar myopathies, the membrane skeleton elements dystrophin and spectrin colocalize with vacuoles (De Bleecker, Engel & Winkelmann, 1993) so it is not implausible that such elements are associated with VLDs or their dynamics.

This work was supported by NSERC of Canada research grants to CEM and to LRM. CR was the recipient of a postdoctoral fellowship from the Ministere francais de la Recherche et de l'Espace. We thank J-M. Trifaro for the use of his image processing equipment.

References

Auer, R.N., Coulter, K.C. 1994. The nature and time course of neuronal vacuolation induced by the NMDA antagonist MK-801. *Acta Neuropath.* **87:**1–7

Baas, P.W., Black, M.M. 1990. Individual microtubules in the axon consist of domains that differ in both composition and stability. *J. Cell. Biol.* **111:**495–509

Block, M.R., Glick, B.S., Wilcox, C.A., Wieland, F.T., Rothman, J.E. 1988. Purification of an N-ethylmaleimide-sensitive protein catalyzing vesicular transport. *Proc. Natl. Acad. Sci. USA* **85:**7852–7856

Bray, D. 1992. Cell Movements. Garland, New York

Bray, D., Money, N.P., Harold, F.M., Bamburg, J.R. 1991. Responses of growth cones to changes in osmolality of the surrounding medium. *J. Cell Science* **98:**507–515

Brett, J., Godman, G.C. 1984. Membrane cycling and macrovacuolation under the influence of cytochalasin: kinetic and morphometric studies. *Tissue & Cell* **16:**325–335

Campenot, R.B. 1984. Inhibition of nerve fiber regeneration in cultured sympathetic neurons by local, high potassium. *Brain Res.* **293:**159–163

Campenot, R.B., Draker, D.D. 1989. Growth of sympathetic nerve

fibers in culture does not require extracellular calcium. *Neuron* **3:**733–743

Cheng, T.P.O., Reese, T.S. 1987. Recycling of plasmalemma in chick tectal growth cones. *J. Neurosci.* **7:**1752–1759

Dailey, M.E., Bridgman, P.C. 1993. Vacuole dynamics in growth cones: correlated EM and video observations. *J. Neurosci.* **13:** 3375–3393

De Bleecker, J.L., Engel, A.G., Windelmann, J.C. 1993. Localization of dystrophin and β-spectrin in vacuolar myopathies. *Am. J. Path.* **143:**1200–1208

Feany, M.B., Buckley, K.M. 1993. The synaptic vesicle protein synaptotagmin promotes formation of filopodia in fibroblasts. *Nature* **364:**537–540

Fishman, H.M., Tewari, K.P., Stein, P.G. 1990. Injury-induced vesiculation and membrane redistribution in squid giantaxon. *Biochem. Biophys. Acta* **1023:**421–435

Gabai, V.L., Kabakov, A.E. 1993. Tumor cell resistance to energy deprivation and hyperthermia can be determined by the actin skeleton stability. *Cancer Letters* **70:**25–31

Goldberg, D.J., Burmeister, D.W. 1992. Microtubule-based filopodial-like protrusions form after axotomy. *J. Neurosci.* **12:**4800–4807

Heidemann, R.R., Buxbaum, R.E. 1994. Mechanical tension as a regulator of axonal development. *Neurotoxicology* **15:**65–108

Heidemann, S.R., Lamoureux, P., Lin, C. 1994. Osmotic stimulation of axonal elongation is mediated by an increase in tension sensitivity of growth. *Am. J. Physiol.* **37:**A12

Hoffman, E.K., Jessen, F., Dunham, P.B. 1994. The Na-K-2Cl cotransporter is in a permanently activated state in cytoplasts from Erlich ascites tumor cells. *J. Membrane Biol.* **138:**229–239

Hoffman, R. 1977. The modulation contrast microscope: principles and performance. *J. Microscopy* **110:**205–222

Kelly, R.B. 1993. A question of endosomes. *Nature* **364:**487–488

Kuznetsov, S.A., Langford, G.M., Weiss, D.G. 1992. Actin-dependent organelle movement in squid axoplasm. *Nature* **356:**722–725

Lamoureux, P., Buxbaum, R.E., Heidemann, S.R. 1989. Direct evidence that growth cones pull. *Nature* **340:**159–162

Lawson, D. 1987. Distribution of myosin and relationship to active organization in cortical and subcortical areas of antibody labelled, quick-frozen, deep-etched fibroblast cytoskeletons. *Cell. Motil. Cytoskel.* **7:**368–380

Lewis, S.A., de Moura, J.L.C. 1982. Incorporation of cytoplasmic vesicles into apical membrane of mammalian urinary bladder epithelium. *Nature* **297:**685–688

Mills, L.R., Neisen, C.E., Kerr, R. 1994. Confocal imaging of living neurons. *In:* Three-dimensional Confocal Microscopy. J.K.S. Stevens, L.R. Mills, J.E. Trogadis, editors. Academic Press, San Diego, CA. (in press)

Mills, L.R., Niesen, C.E., So, A.P., Carlen, P.L., Spigelman, I., Jones, O.T. 1994. N-type Ca^{2+} channels are located on somata, dendrites and a subpopulation of dendritic spines on live hippocampal pyramidal neurons. *J Neurosci. (in press)*

Milton, R.L., Caldwell, J.H. 1990. Na current in membrane blebs: implications for channel mobility patch clamp recording. *J. Neurosci.* **10:**885–893

Morris, C.E., Horn, R. 1991. Failure to elicit neuronal macroscopic mechanosensitive currents anticipated by single channel studies. *Science* **251:**1246–1249

Morris, C.E., Sigurdson, W.J. 1989. Stretch-inactivated ion channels coexist with stretch-activated ion channels. *Science* **243:**807–809

Olney, J.W., Labruyere, J., Wang, G., Wozniak, D.F., Price, M.T., Sesma, M.A. 1991. NMDA antagonist neurotoxicity: mechanism and prevention. *Science* **254:**1515–1518

Popov, S., Brown, A., Poo, M.M. 1993. Forward plasma membrane flow in growing nerve processes. *Science* **259:**244–246

Reaves, B., Banting, G. 1992. Perturbation of the morphology of the trans-golgi network following Brefeldin A treatment: redistribution of a TGN-specific integral membrane protein, TGN38. *J. Cell Biol.* **116:**85–94

Sigurdson, W.J., Morris, C.E. 1989. Stretch-activated ion channels in growth cones of snail neurons. *J. Neurosci.* **9:**2801–2808

Small, D.L., Morris, C.E. (1994) Delayed activation of single mechanosensitive channels in Lymnaea neurons. *Am. J. Physiol.* **267:**C598–C606

Steinhardt, R.A., Bi, G., Alderton, J.M. 1994. Cell membrane resealing by a vesicular mechanism similar to neurotransmitter release. *Science* **263:**390–393

Sukhorukov, V.L., Arnold, W.M., Zimmermann, U. 1993. Hypotonically induced changes in the plasma membrane of cultured mammalian cells. *J. Membrane Biol.* **132:**27–40

Ursitti, J.A., Wade. 1993. Ultrastructure and immunocytochemistry of the isolated human erythrocyte membrane skeleton. *Cell. Motil. Cytoskel.* **25:**30–42

van Rossum, G.D.V., Russo, M.A., Schisselbauer, J.C. 1987. Role of cytoplasmic vesicles in volume maintenance. *Curr. Top. Membr. Transp.* **30:**45–74

Wan, X., Harris, J.A., Morris, C.E. 1995. Responses of neurons to extreme osmomechanical stress. *J. Membrane Biol.* **145:**21–31

Wang, N., Butler, J.P., Ingber, D.E. 1993. Mechanotransduction across the cell surface and through the cytoskeleton. *Science* **260:**1124–1127

Wolfe, J., Dowgert, M.F., Steponkus, P.L. 1984. Dynamics of membrane exchange of the plasma membrane and the lysis of isolated protoplasts during rapid expansions in areas. *J. Membrane Biol.* **86:**127–138

Zheng, J., Buxbaum, R.E., Heidemann, S.R. 1994. Measurements of growth cone adhesion to culture surfaces by micromanipulation. *J. Cell Biol.* **127:**2049–2060